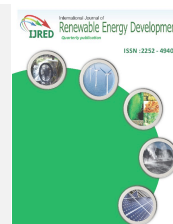




Contents list available at IJRED website

Int. Journal of Renewable Energy Development (IJRED)

Journal homepage: <http://ejournal.undip.ac.id/index.php/ijred>



Research Article

# Optimal Scheduling of Solar-Wind-Thermal Integrated System Using $\alpha$ -Constrained Simplex Method

Sunimerjit Kaur<sup>a\*</sup>, Yadwinder Singh Brar<sup>a</sup>, Jaspreet Singh Dhillon<sup>b</sup>

<sup>a</sup>Department of Electrical Engineering, I.K. Gujral Punjab Technical University, Kapurthala 144603, Punjab, India

<sup>b</sup>Department of Electrical & Instrumentation Engineering, Sant Longowal Institute of Engineering and Technology, Sangrur 148106, Punjab, India

**ABSTRACT.** In this paper, multi-objective economic-environmental solar-wind-thermal power scheduling model is developed. This model is optimized for five test systems. First test system is based upon a purely thermal power generating system. Its problem is formulated to satisfy the three conflicting objectives: (i) fuel cost, (ii)  $NO_x$  emission, and (iii)  $SO_2$  emission. The second, third and fourth test system considers integrated solar-thermal, wind-thermal and solar-wind-thermal power systems, respectively for optimal scheduling. Uncertainty costs are also considered in the renewable power based systems. These four test systems are examined for five power demands i.e. 200 MW, 225 MW, 250 MW, 275 MW, & 300 MW. Fifth test system is also deployed upon a renewable-thermal power scheduling. The effects of variation in number of thermal generators on fuel cost and  $SO_2$  emission are perceived, for a power demand of 400 MW. The value of fuel cost (4067.98 Rs/h) and  $SO_2$  emission (2,441.05 kg/h) is reduced to 3,232.94 Rs/h and 1,939.30 kg/h, respectively, when number of thermal generators are reduced from four to two. The  $\alpha$ -constrained simplex method (ACSM) is used for simulation and the results are compared with simplex method (SM). The results clearly depict the dominance of ACSM over SM in almost all the fields.

**Keywords:** Integrated system, Uncertainty cost, Mutation, Wind farms, Solar units,  $\alpha$ -Constrained Simplex Method

**Article History:** Received: 6<sup>th</sup> August 2020; Revised: 20<sup>th</sup> September 2020; Accepted: 30<sup>th</sup> September 2020; Available online: 5<sup>th</sup> Oct 2020

**How to Cite This Article:** Kaur, S., Brar, Y.S., Dhillon, J.S. (2021) Optimal Scheduling of Solar-Wind-Thermal Integrated System Using  $\alpha$ -Constrained Simplex Method. *International Journal of Renewable Energy Development*, 10(1), 47-59. <https://doi.org/10.14710/ijred.2021.32245>

## 1. Introduction

Some issues regarding fossil fuels like cost, environmental factors, limited resources and rise in power demand etc. have started overweighing their abilities like higher energy density and efficiency etc. In the past decades, researchers started exploring its options. Renewable Energy Resources (RER) have so much power that perhaps one day they can carry all the weight on their tubers. But till now, because of their spasmodic nature, it is difficult to rely completely on RER. Therefore, integrated systems are the only option left.

Mondal *et al.* (2013) presented multi-objective economic emission load dispatch solution using gravitational search algorithm and considering wind power penetration. Hetzer *et al.* (2008) have suggested an economic dispatch model incorporating wind power. Dubey *et al.* (2015a) tested hybrid flower pollination algorithm with time-varying fuzzy selection mechanism for wind integrated multi-objective dynamic economic dispatch. Kayalvizhi and Kumar (2018) have formed stochastic optimal power flow in presence of wind generations by using harmony search algorithm. Damodaran and Kumar (2018) suggested hydro-thermal-wind generation scheduling considering economic and environmental factors with

heuristic algorithms. Li and Kuri (2005) have presented generation scheduling system with wind power. Panda and Tripathy (2016) explored solution of wind integrated thermal generation system for environmental optimal power flow with hybrid algorithm. Tan *et al.* (2019) have worked on optimal scheduling of hydro-PV-wind hybrid system considering CHP and BESS coordination. Tyagi *et al.* (2016) have formulated economic load dispatch of wind-solar-thermal system using backtracking search algorithm. Saxena and Ganguli (2015) have worked on solar and wind power estimation and economic load dispatch using firefly algorithm. Mondal *et al.* (2012) found solution of cost constrained emission dispatch problems considering wind power generation. They have used gravitational search algorithm. Takahama and Sakai (2005) worked on constrained optimization by applying the  $\alpha$ -constrained method to the nonlinear simplex method with mutations. Gangwar and Chishti (2014) have used hybrid simplex method for economic load dispatch. Reddy *et al.* (2016) have demonstrated optimal operation of microgrid using hybrid differential evolution and harmony search algorithm. Reddy (2017a) worked on optimal scheduling of wind-thermal power system using clustered adaptive teaching learning based optimization. Reddy (2017b) suggested optimization of renewable energy

\*Corresponding author: [sunimerriar@yahoo.co.in](mailto:sunimerriar@yahoo.co.in)

resources in hybrid energy systems. Mohamad *et al.* (2019) have worked on hybrid optimization technique for short term wind-solar-hydrothermal generation scheduling. He *et al.* (2019) have elaborated integrated scheduling of hydro, thermal and wind power with spinning reserve. Vaderoqli *et al.* (2020) investigated optimization under uncertainty to reduce the cost of energy for parabolic trough solar power plants with different weather conditions. Correa-Jullian *et al.* (2020) have suggested operation scheduling in a solar thermal system: a reinforcement learning based framework. Nguyen *et al.* (2020) have demonstrated optimal scheduling of large scale wind-hydro-thermal systems with fixed head short term model.

In this paper,  $\alpha$ -Constrained Simplex Method (ACSM) is suggested for optimal scheduling of solar-wind-thermal integrated system. This meta-heuristic technique is a combination of other modes like Nelder and Mead's nonlinear simplex method, mathematical methods, evolutionary method,  $\alpha$ -constrained method etc. (Takahama and Sakai 2005). It is comprised after performing three major improvements in an ordinary simplex method (SM) i.e. (i) using  $\alpha$ -level comparisons instead of ordinary comparisons, (ii) executing mutations of worst points, (iii) creating multi-simplexes instead of a single simplex. ACSM is a very precise, stable and fast technique. Its reliability has been investigated on five test systems.

## 2. Multi Objective Problem Formulation

In this paper, three conflicting objectives of thermal, solar and wind power systems have been considered. These economic environmental objectives are:

- (i). Cost (fuel cost of thermal generating system, overall costs of wind and solar systems)
- (ii).  $NO_x$  pollutant emission
- (iii).  $SO_2$  pollutant emission

Second and third objectives are purely related to thermal generation system.

### 2.1 Economy objective

The economy objective of solar-wind-thermal integrated system (Kothari and Dhillon 2011; Dubey *et al.* 2015b; Sinha *et al.* 2003; Wood and Wollenberg 2006) is:

$$F_1 = \sum_{i=1}^{Gt} (a_{Ti}P_{Ti}^2 + b_{Ti}P_{Ti} + c_{Ti}) + \sum_{j=1}^{Gw} W_{wj} + \sum_{k=1}^{Gs} W_{sk} \quad (Rs/h) \quad (1)$$

Where:

- $Gt$  : number of thermal generators
- $Gw$  : number of wind generators
- $Gs$  : number of solar units
- $P_{Ti}$  : the power output of  $i^{th}$  thermal generator in MW
- $a_{Ti}$ ,  $b_{Ti}$  and  $c_{Ti}$  are cost coefficients of  $i^{th}$  thermal generator
- $W_{wj}$  : the wind power cost of  $j^{th}$  wind generator
- $W_{sk}$  : the solar power cost of  $k^{th}$  solar unit

### 2.2 Environmental objectives

$NO_x$  and  $SO_2$  emissions are given as quadratic functions of thermal power output.  $NO_x$  emission can be evaluated as (Kothari and Dhillon 2011):

$$F_2 = \sum_{i=1}^{Gt} (d_{1i}P_{Ti}^2 + e_{1i}P_{Ti} + f_{1i}) Kg/h \quad (2)$$

Where:

- $d_{1i}$ ,  $e_{1i}$  and  $f_{1i}$  are  $NO_x$  emission coefficients of  $i^{th}$  thermal generator.

$SO_2$  emission can be given by (Kothari and Dhillon 2011):

$$F_3 = \sum_{i=1}^{Gt} (d_{2i}P_{Ti}^2 + e_{2i}P_{Ti} + f_{2i}) Kg/h \quad (3)$$

Where:

- $d_{2i}$ ,  $e_{2i}$  and  $f_{2i}$  are  $SO_2$  emission coefficients of  $i^{th}$  thermal generator.

### 2.3 Multi-objective optimization problem

Minimize  $[F_1, F_2, F_3]^T$

Subject to:

1. The equality constraint (Saxena and Ganguly 2015; Reddy 2017a):

$$\sum_{i=1}^{Gt} P_{Ti} + \sum_{j=1}^{Gw} P_{wj} + \sum_{k=1}^{Gs} P_{sk} = P_D + P_L \quad (4)$$

Where:

- $P_{wj}$  and  $P_{sk}$  are scheduled powers of  $j^{th}$  wind farm and  $k^{th}$  solar unit (MW)
- $P_D$  is power demand (MW)
- $P_L$  is transmission losses (MW)

2. Power generation limits on thermal, wind and solar units (Saxena and Ganguly 2015; Reddy 2017a):

$$P_{T_{i_{min}}} \leq P_{Ti} \leq P_{T_{i_{max}}} \quad (i = 1, 2, \dots, Gt) \quad (5)$$

$$0 \leq P_{wj} \leq P_{wRj} \quad (j = 1, 2, \dots, Gw) \quad (6)$$

$$0 \leq P_{sk} \leq P_{sRk} \quad (k = 1, 2, \dots, Gs) \quad (7)$$

Where:

- $P_{T_{i_{min}}}$  and  $P_{T_{i_{max}}}$  are lower and upper limits of power output of  $i^{th}$  thermal generator in MW, respectively
- $P_{wRj}$  is rated power output of  $j^{th}$  wind farm in MW
- $P_{sRk}$  is rated power output of  $k^{th}$  solar unit in MW

### 2.4 Model of solar power uncertainty

Sun is continuously generating heat by thermo-nuclear fusion reactions, in which hydrogen atoms are converted into helium atoms and the evolved energy is radiated in all directions. Earth and its atmosphere is continuously receiving  $1.7 \times 10^{17}$  W of radiations (Singal 2006). It is a very small fraction of total energy radiated by the sun. The

quantity and quality of radiations that reaches the earth depends upon the geographical location and weather conditions of a particular area. The power output of solar unit can be expressed as (Tan *et al.* 2019):

$$P_{avs} = P_{SR} I_T \frac{(1 + k_a(T_c - T_r))}{I_{sc}} \quad (8)$$

Where:

- $P_{SR}$  : the rated power of solar unit (MW)
- $T_c$  : the operating temperature (°C)
- $T_r$  : the reference temperature (°C)
- $k_a$  : the temperature coefficient (°C)
- $I_{sc}$  : maximum value of solar radiations incident under standard conditions (MJ/m<sup>2</sup>-h)

The hourly beam solar radiations incident on an inclined plane at northern hemisphere (Singal 2006) is:

$$I_T = \frac{I_b \cos \theta_c}{\cos \theta} \quad (9)$$

$$= \frac{I_b [\cos(\theta - \beta_1) \cos \delta \cos \omega + \sin(\theta - \beta_1) \sin \delta]}{(\cos \delta \cos \omega \cos \theta + \sin \theta \cos \delta)} \quad (10)$$

Where:

- $\beta_1$  :  $\theta \pm 15^\circ$
- $I_b$  : hourly beam solar radiation incident on a horizontal plane(MJ/m<sup>2</sup>-h)
- $\theta$  : angle of incidence of beam solar radiation on horizontal plane (°)
- $\theta_c$  : angle of incidence of beam solar radiation on tilted solar collector towards equator (°)
- $\beta_1$  : angle of tilt of solar collector (°)
- $\delta$  : sun's declination (°)
- $\omega$  : hour angel (°)
- $d$  : the day of the year

Angle of sun's declination can be calculated as (Singal, 2009):

$$\delta = 23.45^\circ \sin\left(\frac{360(284 + d)}{365}\right) \quad (10.1)$$

Due to uncertain behavior of solar radiations, the total operating solar power cost consists of two parts i.e. (i) direct cost (ii) uncertainty cost. Uncertainty cost comprises (a) overestimation cost (b) underestimation cost. Therefore, total operating cost of solar power is given as:

$$\sum_{k=1}^{Gs} W_{Sk} = \sum_{k=1}^{Gs} (E_{Sk} + E_{osk} + E_{usk}) \quad (11)$$

Where:

- $E_{Sk}$  : the direct cost function of  $k^{th}$  solar units
- $E_{osk}$  : the overestimation cost function of  $k^{th}$  solar units
- $E_{usk}$  : the underestimation cost function of  $k^{th}$  solar units

Direct cost is a linear cost function of scheduled solar power. It can be determined as:

$$\text{Direct cost} = \sum_{k=1}^{Gs} (E_{ck} P_{sk}) \quad (12)$$

Where:

- $E_{ck}$  : the direct cost coefficient of  $k^{th}$  solar unit.

If the available solar power is less than the estimated value then operator has to purchase some power from any different source. This extra cost is called overestimation cost and it can be calculated as:

$$\text{Overestimation cost} = \sum_{k=1}^{Gs} (E_{ock} (P_{sk} - P_{avsk})) \quad (12.1)$$

Where:

- $E_{osk}$  : the overestimation cost coefficient of  $k^{th}$  solar unit.

If the available solar power is more than the estimated value then extra power is wasted. Therefore, operator has to compensate the supplier's cost. This compensated value is called underestimation cost and it can be evaluated as:

$$\text{Underestimation cost} = \sum_{k=1}^{Gs} (E_{uck} (P_{avsk} - P_{sk})) \quad (12.2)$$

Where:

- $E_{usk}$  : the underestimation cost coefficient of  $k^{th}$  solar unit.

### 2.5 Model of wind power uncertainty

Output power of wind generators depends upon wind strength of the particular area, which is completely unpredictable. Therefore, it is not possible to accurately forecast wind characteristics. Weibull distribution density factor can be used to analyze wind data. Wind speed frequency distribution can display a clear picture of wind energy potential in a specific area. It can be formulated as (Reddy *et al.* 2016; Reddy 2017b):

$$F_v = \left(\frac{k}{c}\right) \left(\frac{v}{c}\right)^{k-1} \exp\left[-\left(\frac{v}{c}\right)^k\right], \quad (0 \leq v \leq \infty) \quad (13)$$

Where:

- $k$ : the Weibull shape factor
- $c$ : the Weibull scale factor
- $v$ : the annual average speed in m/sec

The wind power generated at different wind velocities can be expressed as (Reddy *et al.* 2016):

$$P_{avw} = \begin{cases} 0 & ; \text{for } v < v_i \text{ and } v > v_o \\ \frac{P_{wrj}(v - v_i)}{(v_r - v_i)} & ; \text{for } v_i < v < v_r \\ P_{wrj} & ; \text{for } v_r \leq v \leq v_o \end{cases} \quad (14)$$

Where:

- $v_i$ : cut in speed of wind generator in m/sec

- $v_r$ : rated speed of wind generator in m/sec
- $v_o$ : cut out speed of wind generator in m/sec

It means that wind power is zero, when wind speed is less than cut in speed or greater than cut out speed. Wind power becomes equal to rated power of  $j^{th}$  wind generator, when wind speed lies between rated wind speed and cut out speed. The probability of wind power can be calculated as (Saxena and Ganguly 2015):

$$f(P_{avw}) = \begin{cases} \left(\frac{klv_i}{c}\right)\left(\frac{(1+\rho l)v_i}{c}\right)^{k-1} \exp\left[-\left(\frac{(1+\rho l)v_i}{c}\right)^k\right] & ; \text{for } 0 < v < v_r \\ 1 - \exp\left[-\left(\frac{v_r}{c}\right)^k\right] + \exp\left[-\left(\frac{v_o}{c}\right)^k\right] & ; \text{for } v = 0 \\ \exp\left[-\left(\frac{v_r}{c}\right)^k\right] - \exp\left[-\left(\frac{v_o}{c}\right)^k\right] & ; \text{for } v = v_r \end{cases} \quad (15)$$

Where:

- $\rho = \frac{v}{v_r}$  and  $l = \frac{(v_r - v_i)}{v_i}$

Also, the total operating cost of wind power composes of (1) direct cost, (2) uncertainty cost. The direct cost of wind power generation is (Reddy *et al.* 2016; Reddy 2017a):

$$C_{dj} = C_{aj}P_{wj} \quad (16)$$

Where:

- $C_{aj}$  is direct cost coefficient of  $j^{th}$  wind generator.

Further the conditions for uncertainty are verified to obtain uncertainty cost. If available wind power is less than scheduled wind power, then overestimation cost is (Reddy 2017a; Kayalvizhi and Kumar 2018):

$$C_{oj} = C_{owj} \int_0^{P_{wj}} (P_{wj} - P_{avw}) f(P_{avw}) d(P_{avw}) \quad (17)$$

Where:

- $C_{owj}$  : the overestimation cost coefficient of  $j^{th}$  wind generator.

When available wind power is more than scheduled wind power, then underestimation cost is (Kayalvizhi & Kumar 2018):

$$C_{uj} = C_{pwj} \int_0^{P_{wj}} (P_{avw} - P_{wj}) f(P_{avw}) d(P_{avw}) \quad (18)$$

Where:

- $C_{pwj}$  : the underestimation cost coefficient of  $j^{th}$  wind generator.

$$\text{Total wind generation cost} = \text{direct cost} + \text{uncertainty cost} \quad (19)$$

In this paper, uncertainty cost of wind power is determined after verifying the uncertainty conditions. In

case of overestimation of wind power, only overestimation cost is calculated as uncertainty cost and in case of underestimation of wind power, only underestimation cost is evaluated as uncertainty cost.

### 2.6 Transmission losses

System transmission losses are evaluated by using Kron's approximated loss formula through  $B$ -coefficients. In this paper, transmission losses are calculated separately for thermal, solar and wind systems and then added together. If  $P_{LT}$ ,  $P_{LS}$  and  $P_{Lw}$  are losses due to thermal, solar and wind systems and  $B_{ij}$  are the  $B$ -coefficients, then (Kothari & Dhillon 2011):

$$P_{LT} = \sum_{i=1}^{Gt} \left( \sum_{j=1}^{Gt} P_{Ti} B_{Tij} P_{Tj} \right) \quad (20)$$

$$P_{LS} = \sum_{i=1}^{Gs} \left( \sum_{j=1}^{Gs} P_{Si} B_{Sij} P_{Sj} \right) \quad (21)$$

$$P_{Lw} = \sum_{i=1}^{Gw} \left( \sum_{j=1}^{Gw} P_{Wi} B_{Wij} P_{Wj} \right) \quad (22)$$

Total transmission losses of the system are:

$$P_L = P_{LT} + P_{LS} + P_{Lw} \quad (23)$$

### 3. Solution Methodology

In 1965, Nelder and Mead fabricated nonlinear Simplex Method (SM), which is a direct search technique for function minimization. In this method for ' $n$ ' objectives,  $n+1$  points are searched for a search space ' $S$ ' to create a non-zero initial volume simplex. If  $X^y$  denotes each vertex of the simplex (where  $y = 1, 2, \dots, n+1$ ), then worst point (least desirable point) of initial simplex is found. Then using fixed rules, new simplex is formed from old simplex in such a way that navigates search away from worst point in the simplex. The entire process is explored by using three operations i.e. reflection, expansion & contraction. This activity continues until the simplex is sufficiently converged.

SM has many limitations, therefore ACSM has been introduced (Takahami and Sakai 2005). This is a modified form of SM as given below:

- Replacement of ordinary comparisons by  $\alpha$ -level comparisons:

Ordinary comparisons of SM are replaced by  $\alpha$ -level comparisons to convert an unconstrained optimization technique to a constrained optimization technique. Here, constraint violations and objective functions are treated separately. That is, points are compared on the basis of their constraint violation.

- Use of boundary mutations and multi- simplexes: Sometimes during reduction process of simplex, few points around the boundary of feasible region are omitted. Therefore the boundary mutation of the worst point and

multi-simplexes are used to search the borderline of feasible region in ACSM.

3.1 Algorithm of ACSM

Let  $x = [X^1, X^2, \dots, X^n]^T$  is an n-dimensional vector of decision variables and feasible solutions exists in the search space 'S'. Consider  $f(x)$  is the objective function. Let expansion factor  $\gamma > 1$ , contraction factor  $b \in (0, 1)$ , tolerance limit  $\varepsilon = 0.001$  and mutation rate  $P_b \in (0 - 1)$ . Following points describes this algorithm of  $\alpha$ -constrained simplex method:

1). Population Generation:

Generate initial population  $N (> n + 1)$ , in the form of search points.  $n+1$  points are required to compose one simplex. However, to generate more than one simplex, N number of points are required.

2). Evaluation of Points:

Find  $X^l$ (best point/ most desirable point),  $X^h$  (worst point/ least desirable point) and  $X^s$  (next to worst point/ second worst point) from the following equations:

$$X^l = \arg \min_i f(x^i)$$

$$X^h = \arg \max_i f(x^i)$$

$$X^s = \arg \max_{i \neq h} f(x^i)$$

3). Mutation of worst point:

Produce random number  $R$  and update  $X^h$  as:

$$X^h = \begin{cases} X^l + R(X^h - X^l) & ; R_n \geq P_b \\ X^h - R(X^h - X^l) & ; \text{otherwise} \end{cases}$$

4). Formulation of initial simplex:

Omit the worst point  $X^h$  and create initial simplex using  $n+1$  points.

5). Calculation of centroid:

To find a new search point in place of worst point, centroid of other points (excluding worst point) is calculated as:

$$X^0 = \frac{1}{n+1} \sum_{i=1}^{n+1} X^i$$

6). Calculation of reflected point:

To find the reflected point, the worst point is reflected about the centroid (with the help of  $\alpha$  obtained from Eq. 24). It is given as:

$$X^r = (1 + \alpha)X^0 - \alpha X^h$$

7).  $\alpha$  –level comparisons:

- (i). If  $X^r$  is better than the best point i.e.  $f(X^r, \mu_\alpha(X^r)) <_\alpha f(X^l, \mu_\alpha(X^l))$ , then go to step (ii), else go to step (iii). Here  $\mu_\alpha(x)$  is the satisfaction level of membership function (Eq. 26).
- (ii). Calculate expansion point  $X^e$  as:

$$X^e = \gamma X^r + (1 - \gamma)X^0$$

If  $X^e$  is better than  $X^l$ , then  $X^h = X^e$ , else  $X^h = X^r$  and go back to step 2.

- (iii). If  $X^r$  is better than or equal to  $X^s$ , then  $X^h = X^r$  and go back to step 2, else go to step (iv).
- (iv). If  $X^r$  is better than  $X^h$ , then  $X^h = X^r$ .
- (v). Evaluate contraction point  $X^c$ :

$$X^c = bX^h + (1 - b)X^0$$

If  $X^c$  is better than  $X^h$ , then  $X^h = X^c$ , otherwise

$$X^h = bX^h + (1 - b)X^l$$

and go back to step 2.

8). Stopping criterion:

If  $\text{abs}(f^l - f^h) \leq \varepsilon$  then go to step 9, else go to step 2.

9). Stop.

3.2 Calculation of alpha-a

Generally, it is not required to control the  $\alpha$ -level. For constrained problems, which are based on lexicographic order, value of  $\alpha$ -level is set to 1. But for the problems having very small feasible regions (such as problems with equality constrained), controlled  $\alpha$  value gives good solutions. Its value lies between 0–1. It can be found as (Takahama and Sakai 2005):

$$\alpha(t) = \begin{cases} \frac{1}{2} \left( \max(\mu_\alpha(X^t)) + \frac{1}{N} \sum_{i=1}^N \mu_\alpha(X^i) \right) ; t = 0 \\ (1 - \beta)\alpha(t - 1) + \beta ; 0 < t \leq \frac{T_{max}}{2} \text{ and } (t \bmod T_\alpha) = 0 \\ \alpha(t - 1) ; 0 < t \leq \frac{T_{max}}{2} \text{ and } (t \bmod T_\alpha) \neq 0 \\ 1 ; t > \frac{T_{max}}{2} \end{cases} \quad (24)$$

Where:

- $t$  : the number of iterations
- $T_{max}$ : the maximum number of iterations

The value of  $\alpha$  can be controlled by using  $\beta = 0.03$  and  $T_\alpha = 50$ . The first value of  $\alpha$  is the average of the best satisfaction level and average of all satisfaction levels. Now the minimum constraint violation solutions are obtained as:

- (a) the value of  $\alpha$  is updated as per (24) for the condition the number of iterations ( $t$ ) are multiple of  $T_\alpha$ .
- (b) the value of  $\alpha$  is set to be 1 for the condition the ( $t$ ) exceeds  $\frac{T_{max}}{2}$ .

4. Decision Making

It is assumed that decision making has an inexplicit nature and fuzzy goals for objective functions (Kothari and Dhillon 2011; Dhillon et al. 2002). To find the most suitable solution from the non-inferior solutions the fuzzy satisfying method is used. Fuzzy goal for each objective

function is set by defining their membership functions, which are assumed to be strictly monotonically decreasing and continuous functions. Their membership values vary from 0–1. The value ‘0’ of membership function means incompatibility, whereas value ‘1’ designates complete compatibility. It is defined as (Kothari and Dhillon 2011; Reddy *et al.* 2011; Reddy *et al.* 2015):

$$\mu(F_i) = \begin{cases} 1 & ; F_i \leq F_i^{min} \\ \frac{F_i^{max} - F_i}{F_i^{max} - F_i^{min}} & ; F_i^{min} < F_i < F_i^{max} \\ 0 & ; F_i \geq F_i^{max} \end{cases} \quad (25)$$

$i=1,2,\dots,M$

Here:

- $F_i$ ,  $F_i^{max}$  and  $F_i^{min}$  are the objective function, maximum value of objective function and minimum value of objective function, respectively.

For completion of each non dominated solution, in satisfying the objectives, addition of all the values of membership functions is required (for k number of non-

dominated solutions). The efficacy of each non dominated solution can be rated with respect to all non-dominated solutions by normalizing its values of its total addition. It is given by (Kothari and Dhillon 2011; Reddy *et al.* 2011; Reddy *et al.* 2015):

$$\mu_d^k = \frac{\sum_{i=1}^M \mu(F_i^k)}{\sum_{k=1}^K \sum_{i=1}^M \mu(F_i^k)} \quad (26)$$

The function  $\mu_d^k$  can be considered as a membership function of non-dominated solution to a fuzzy set. It is called fuzzy cardinal priority ranking of the non-dominated solutions.

### 5. Test Systems and Results

To illustrate the credibility of suggested method, following five test systems have been observed by using FORTRAN 90 programming language (Mayo 1995). First test system is purely thermal generation system, where as others are integrated with renewable systems. These systems are categorized as:

**Table 1**

The characteristic fuel cost,  $NO_x$  emission and  $SO_2$  emission functions of four thermal generators

Fuel cost (Rs/h) equations	$NO_x$ emission (kg/h) equations	$SO_2$ emission (kg/h) equations
$F_{11} = 0.002035 P_{T1}^2 + 8.43205 P_{T1} + 85.6348$	$F_{21} = 0.006323 P_{T1}^2 - 0.38128 P_{T1} + 80.9019$	$F_{31} = 0.001206 P_{T1}^2 + 5.05928 P_{T1} + 51.3778$
$F_{12} = 0.003866 P_{T2}^2 + 6.41031 P_{T2} + 303.7780$	$F_{22} = 0.006483 P_{T2}^2 - 0.79027 P_{T2} + 28.8249$	$F_{32} = 0.002320 P_{T2}^2 + 3.84624 P_{T2} + 182.2605$
$F_{13} = 0.005963 P_{T3}^2 + 6.91559 P_{T3} + 202.0258$	$F_{23} = 0.006181 P_{T3}^2 - 0.39077 P_{T3} + 50.3808$	$F_{33} = 0.003578 P_{T3}^2 + 4.14938 P_{T3} + 121.2133$
$F_{14} = 0.001345 P_{T4}^2 + 8.30154 P_{T4} + 274.2241$	$F_{24} = 0.006732 P_{T4}^2 - 2.39928 P_{T4} + 610.2535$	$F_{34} = 0.000813 P_{T4}^2 + 4.97641 P_{T4} + 165.3433$

**Table 2**

Solution of power scheduling problem with three thermal generators using ACSM

Output variables	200 MW	225 MW	250 MW	275 MW	300 MW
$P_{T1}$ (MW)	68.12	76.73	85.31	93.96	102.71
$P_{T2}$ (MW)	67.74	76.35	84.93	93.58	102.33
$P_{T3}$ (MW)	66.98	75.59	84.16	92.81	101.56
Min fuel cost - Gt1 (Rs/h)	661.07	736.17	811.26	887.35	964.56
Min fuel cost - Gt2 (Rs/h)	750.31	811.06	870.50	931.88	994.51
Min fuel cost - Gt3 (Rs/h)	692.00	758.85	826.32	895.29	965.90
BCS fuel cost - Gt1 (Rs/h)	669.53	744.68	819.82	895.95	973.22
BCS fuel cost - Gt2 (Rs/h)	755.81	815.80	876.12	937.57	1000.27
BCS fuel cost - Gt3 (Rs/h)	692.00	758.85	826.32	895.29	965.90
BCS total fuel cost (Rs/h)	2117.36	2319.35	2522.27	2728.82	2939.40
Min $NO_x$ emission (kg/h) Gt1	83.81	88.31	93.72	100.12	107.55
Min $NO_x$ emission (kg/h) Gt2	04.97	06.19	8.26	11.31	15.42
Min $NO_x$ emission (kg/h) Gt3	50.38	50.38	50.38	67.36	50.38
BCS $NO_x$ emission (kg/h) - Gt1	84.27	88.87	94.39	100.90	108.45
BCS $NO_x$ emission (kg/h) - Gt2	5.04	6.28	8.47	11.64	15.84
BCS $NO_x$ emission (kg/h) - Gt3	51.93	56.16	61.27	67.36	74.45
BCS Total $NO_x$ emission (kg/h)	141.25	151.31	164.14	179.91	198.74
Min. $SO_2$ emission (kg/h) - Gt1	396.57	441.61	486.65	532.28	578.58
Min. $SO_2$ emission (kg/h) - Gt2	450.18	488.35	522.79	561.04	596.71
Min. $SO_2$ emission (kg/h) - Gt3	415.20	455.31	495.79	537.17	580.35
BCS $SO_2$ emission (kg/h) - Gt1	401.65	446.72	491.78	537.44	1763.49
BCS $SO_2$ emission (kg/h) - Gt2	453.48	489.48	525.67	562.54	583.78
BCS $SO_2$ emission (kg/h) - Gt3	415.20	455.31	495.79	537.17	600.16
BCS total $SO_2$ emission (kg/h)	1270.34	1391.52	1513.25	1637.16	579.54
Transmission losses (MW)	2.80	3.55	4.40	5.34	6.39
Simulation time(sec)	0.51	0.51	0.51	0.52	0.52

**Table 3**  
Solution of power scheduling problem with three thermal generators using SM

Output Variables	200 MW	225 MW	250 MW	275 MW	300 MW
$P_{T1}$ (MW)	68.19	76.81	85.39	94.06	102.82
$P_{T2}$ (MW)	67.81	76.43	85.01	93.68	102.43
$P_{T3}$ (MW)	67.04	75.66	84.24	92.91	101.66
Min fuel cost - Gt1 (Rs/h)	661.73	736.90	812.07	888.23	965.52
Min fuel cost - Gt2 (Rs/h)	751.06	811.87	871.37	932.81	995.51
Min fuel cost - Gt3 (Rs/h)	692.69	759.61	827.14	896.18	966.87
BCS fuel cost - Gt1 (Rs/h)	670.20	745.43	820.64	896.85	974.20
BCS fuel cost - Gt2 (Rs/h)	756.57	816.62	877.00	938.51	1,001.27
BCS fuel cost - Gt3 (Rs/h)	692.69	759.61	827.14	896.18	966.87
BCS total fuel cost (Rs/h)	2,119.47	2,321.67	2,524.79	2,731.55	2,942.34
Min. $NO_x$ emission (kg/h) - Gt1	83.89	88.39	93.81	100.22	107.66
Min. $NO_x$ emission (kg/h) - Gt2	04.98	06.20	08.27	11.32	15.43
Min. $NO_x$ emission (kg/h) - Gt3	50.43	50.63	50.43	67.42	50.43
BCS $NO_x$ emission (kg/h) - Gt1	84.35	88.96	94.49	101.00	108.55
BCS $NO_x$ emission (kg/h) - Gt2	05.04	06.28	08.47	11.65	15.86
BCS $NO_x$ emission (kg/h) - Gt3	51.99	56.21	61.33	67.42	74.52
BCS total $NO_x$ emission (kg/h)	141.39	151.47	164.30	180.09	198.94
Min $SO_2$ emission (kg/h) - Gt1	396.97	442.05	487.14	532.81	579.16
Min $SO_2$ emission (kg/h) - Gt2	450.63	488.84	523.32	561.60	596.59
Min $SO_2$ emission (kg/h) - Gt3	415.61	455.77	496.28	537.71	580.93
BCS $SO_2$ emission (kg/h) - Gt1	402.05	447.17	492.27	537.98	584.36
BCS $SO_2$ emission (kg/h) - Gt2	453.94	489.97	526.20	563.10	600.76
BCS $SO_2$ emission (kg/h) - Gt3	415.61	455.77	496.28	537.71	580.12
BCS Total $SO_2$ emission (kg/h)	1,271.61	1,392.91	1,514.77	1,638.80	1,765.25
Transmission losses (MW)	2.80	3.56	4.40	5.35	6.39
Simulation time (sec)	0.60	0.60	0.62	0.62	0.62

- Power scheduling with three thermal generators
- Power scheduling with three thermal generators and two wind farms
- Power scheduling with three thermal generators and two solar units
- Power scheduling with three thermal generators, one solar unit and one wind farm
- Power scheduling of a composite system

well as for the whole system. The results are depicted in Table 3.

5.1 Test system 1

It comprises multi-objective thermal power scheduling which minimizes fuel costs and emissions ( $NO_x, SO_2$ ) simultaneously. This system contains three thermal generators i.e.  $Gt1, Gt2$  and  $Gt3$ . Their fuel costs and emission ( $NO_x, SO_2$ ) functions are given in Table 1. Minimum and maximum generation limits for each generator are considered as 10 MW and 250 MW, respectively. Problem is solved for five different power demands (200 MW, 225 MW, 250 MW, 275 MW and 300 MW) using ACSM. Values for the  $\alpha$  are calculated by using Eq. 24. Minimum & best compromised solutions (BCS) of fuel costs and emissions ( $NO_x, SO_2$ ) are evaluated from Eq. (1) to Eq. (3), respectively. Transmission losses are computed by using Eq. 20. Results from Table 2 show that most of the time the values of minimum output variables are either equal to BCS values or the differences between them are very narrow. It happens because, to find the optimal solution, initially simplex is spanned by multiple search points but when it is gradually reduced, the better points are observed inside the simplex. Therefore, at the end when simplex is sufficiently reduced, high quality solutions are observed. The above problem is then solved by utilizing an ordinary SM. Minimum fuel costs, BCS fuel costs, minimum values of emissions ( $NO_x, SO_2$ ) and BCS emissions ( $NO_x, SO_2$ ) are calculated for each generator as

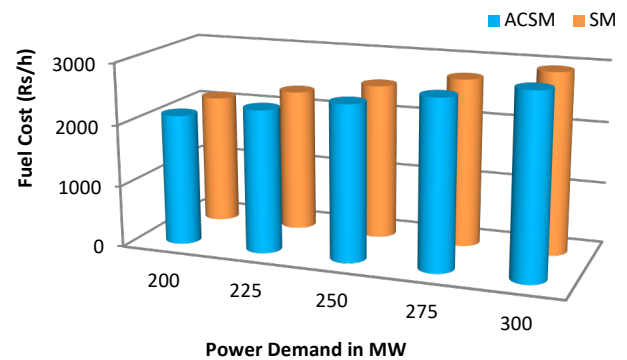


Fig. 1 Comparison of Fuel Costs using ACSM & SM

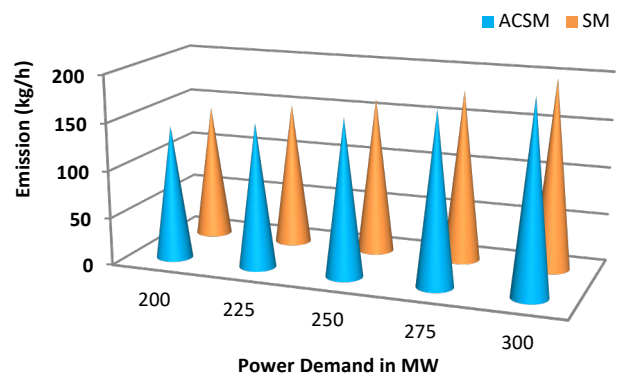


Fig. 2 Comparison of  $NO_x$  emission using ACSM & SM

Fig. 1 presents the comparison of fuel costs using ACSM and SM at various power demands for test system 1. ACSM shows its superiority over SM for each individual power demand through the length of the bars. It can be seen clearly that difference between the values of fuel cost is increasing continuously with the rise in power demand. Fig. 2 compares values of emissions ( $NO_x$ ) evaluated by ACSM and SM. It has been proved that ACSM has overpowered SM with better out-turns in less time. Outcomes clearly depict the supremacy of ACSM over SM.

5.2 Test system 2

It involves power scheduling of solar-thermal integrated system. The system has three thermal and two solar units. It is considered that solar units are placed at New Delhi (India) and time is taken as 1 pm of 15<sup>th</sup> day of June. The geographical latitude is 28.6°, hour angle is 15° and radiation per hour on a horizontal plane is 2.5 MJ/m<sup>2</sup>-h. Parameters of solar units are given in Table 4 (Tyagi *et al.* 2016; Saxena and Ganguly 2015; Singal 2009).

As the 15<sup>th</sup> day of June is the 166<sup>th</sup> day of the year, so angle for sun's declination can be calculated from Eq. (10.1). The hourly beam solar radiations incident on an inclined plane is evaluated from Eq. (10). Then available power from solar units is calculated by using Eq. (8). Total operating cost of the solar power, direct cost, overestimation cost and underestimation cost are computed from Eqs. (11), (12), (12.1) and (12.2), respectively.

The effect of overestimation and underestimation can be clearly found from Table 5. If the available solar power is less than scheduled solar power then overestimation

cost has positive value and underestimation cost has negative value and vice versa. Fig. 3 displays variations of direct cost, overestimation cost and underestimation cost of solar power system with solar scheduled power. It can be seen that the direct cost and the overestimation cost are enhancing, while the underestimation cost is decreasing linearly with increase in solar scheduled power. From Eqs. (12.1) and (12.2), it can be found that the overestimation cost and the under-estimation cost depends upon the difference between scheduled solar power and available solar power. When both the powers become equal to each other (and = 29.295 MW), the value of both uncertainty costs becomes zero and total cost depends only upon direct cost.

Table 4  
Parameters of solar units (PV)

Solar system variables	Specifications
Capacity of each solar unit	30 MW
Temperature coefficient - $K_a$	$-4.7e^{-3} / ^\circ C$
Reference temperature - $T_R$	25 °C
Geographical latitude - $\theta$	28.6° N (For New Delhi)
Sun's declination over the year	-23.45° to 23.45°
hour angle - $\omega$	-15° (at 1 PM)
Angle of tilt of solar collector - $\beta_1$	20°
Coefficient of direct cost	5.0 Rs/kWh
Coefficient of the underestimation cost	17.28 Rs/kWh
Coefficient of the overestimation cost	12.28 Rs/kWh
Radiation per hour on a horizontal plane	2.5 MJ/m <sup>2</sup> -h
Angle of sun's declination	23.3°

Table 5  
Solution of power scheduling problem with three thermal generators and two solar units using ACSM

Output variables	200 MW	225 MW	250 MW	275 MW	300 MW
$P_{T1}$ (MW)	47.58	56.17	64.63	73.66	82.46
$P_{T2}$ (MW)	48.08	55.81	64.97	73.27	82.23
$P_{T3}$ (MW)	47.54	56.15	65.02	73.63	82.89
$P_{S1}$ (MW)	28.67	29.27	28.92	28.85	28.45
$P_{S2}$ (MW)	29.87	29.89	29.32	29.35	28.57
BCS fuel cost - Gt1 (Rs/h)	491.45	565.73	639.17	717.80	794.84
BCS fuel cost - Gt2 (Rs/h)	620.98	673.62	736.61	794.26	857.08
BCS fuel cost - Gt3 (Rs/h)	544.27	609.15	676.95	743.59	816.25
BCS total fuel Cost (Rs/h)	1,656.71	1,848.50	2,052.73	2,255.66	2,468.17
BCS $NO_x$ emission (kg/h) - Gt1	77.07	79.43	82.67	87.12	92.46
BCS $NO_x$ emission (kg/h) - Gt2	5.81	4.91	4.84	5.72	7.67
BCS $NO_x$ emission (kg/h) - Gt3	45.77	47.92	51.10	55.12	60.45
BCS Total $NO_x$ emission (kg/h)	128.66	132.27	138.62	147.97	160.59
BCS $SO_2$ emission (kg/h) - Gt1	294.83	339.39	383.44	430.60	476.80
BCS $SO_2$ emission (kg/h) - Gt2	372.58	404.17	441.96	476.55	514.24
BCS $SO_2$ emission (kg/h) - Gt3	326.56	365.49	406.17	446.15	489.75
BCS Total $SO_2$ emission (kg/h)	993.98	1,109.05	1,231.57	1,353.31	1,480.80
Solar power available (MW)	29.29	29.29	29.29	29.29	29.29
Direct cost $P_{S1}$ (Rs/h)	143,351.85	146,351.65	144,649.45	144,275.50	142,259.95
Direct cost $P_{S2}$ (Rs/h)	149,351.00	149,467.90	146,614.65	146,788.65	142,878.35
Total direct cost (Rs/h)	29,2702.85	29,5819.55	291,264.10	291,064.15	285,138.30
Underestimation cost $P_{S1}$ (Rs/h)	10,793.54	426.29	6309.04	7,601.39	14,567.25
Underestimation cost $P_{S2}$ (Rs/h)	-9,939.54	-10,343.52	-482.58	-1,083.95	12,429.95
Total Underestimation cost (Rs/h)	854.00	-9917.22	5,826.45	6,517.44	26,997.20
Overestimation cost $P_{S1}$ (Rs/h)	-7,670.40	-302.94	-4,483.50	-5,401.91	-10,352.19
Overestimation cost $P_{S2}$ (Rs/h)	7,063.51	7,350.60	342.94	770.31	-8,833.32
Total overestimation Cost (Rs/h)	-606.89	7,047.65	-4,140.56	-4,631.60	-19,185.51
Total cost (Rs/h)- Gs1	146,474.98	146,474.99	146,474.98	146,474.97	146,475.01
Total cost (Rs/h)- Gs2	146,474.97	146,474.98	146,475.01	146,475.00	146,474.97
Total solar generation cost (Rs/h)	292,949.95	292,949.98	292,949.99	292,949.98	292,949.98
Transmission losses (MW)	1.75	2.27	2.91	3.64	4.47
Simulation time (Sec)	0.82	0.82	0.84	0.84	0.84

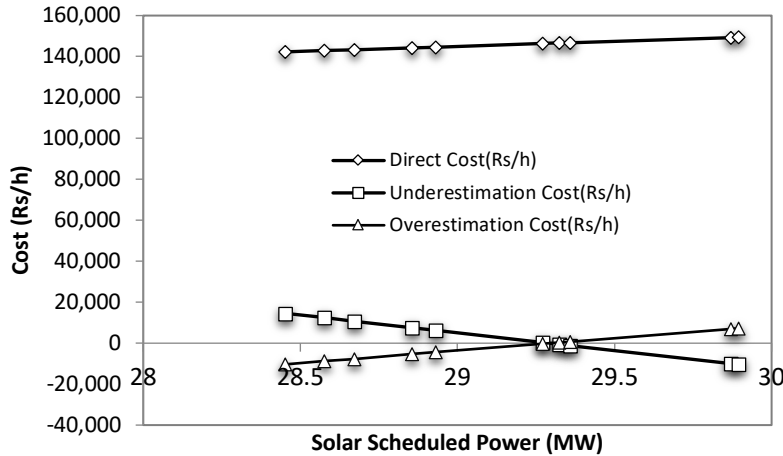


Fig. 3 Variation of solar direct cost, overestimation cost and underestimation cost with scheduled solar power

5.3 Test System 3

It includes a multi-objective power scheduling of wind thermal integrated system. This system contains total five generators i.e. three thermal generators and two wind farms. To observe the wind character, Weibull distribution density factor is taken. Values of shape factor 'k' and scale factor 'c' are taken as 1 and 15 m/sec respectively. Parameters of wind generators are given in the Table 6. Power available from wind generator is found by using Eq. (14) and probability of wind power is computed by using Eq. (15). Direct cost of wind power is obtained from Eq. (16). To calculate the wind uncertainty cost, conditions of overestimation or underestimation are verified. If scheduled wind power is greater than actual wind power then overestimation cost is determined from Eq. (17) and if scheduled wind power is less than actual wind power then underestimation cost is evaluated from Eq. (18). Total operating cost of wind power is found from Eq. (19).

Results of the system are presented in the Table 7. Uncertainty cost of wind depends upon the condition of overestimation or underestimation. Total wind power cost is the sum of direct cost and wind uncertainty cost. Fig. 4 conveys variation of wind direct cost and wind uncertainty cost with wind scheduled power. Direct cost rises with rise

in wind scheduled power, whereas wind uncertainty cost is falling down as the wind scheduled power is getting closer to available wind power. In this paper, operating wind speed is considered as 15 m/sec, therefore the available wind power is 30 MW. Uncertainty cost is directly proportional to the difference between available wind power and scheduled wind power (Eq. 17 and Eq. 18). When scheduled power becomes equal to 30 MW, uncertainty cost becomes zero and overall cost depends only upon direct wind cost (Eq. 19).

Table 6 Parameters of wind generators

Wind system variables	Specifications
Capacity of each wind farm	30 MW
Cut in velocity $v_i$	3.5 m/sec
Cut out velocity $v_o$	25 m/sec
Rated speed $v_r$	15 m/sec
Scale factor $c$	15 m/sec
Shape factor $k$	1
Coefficient of direct cost	4.89 Rs/kWh
Coefficient of underestimation cost	17.28 Rs/kWh
Coefficient of overestimation cost	12.28 Rs/kWh

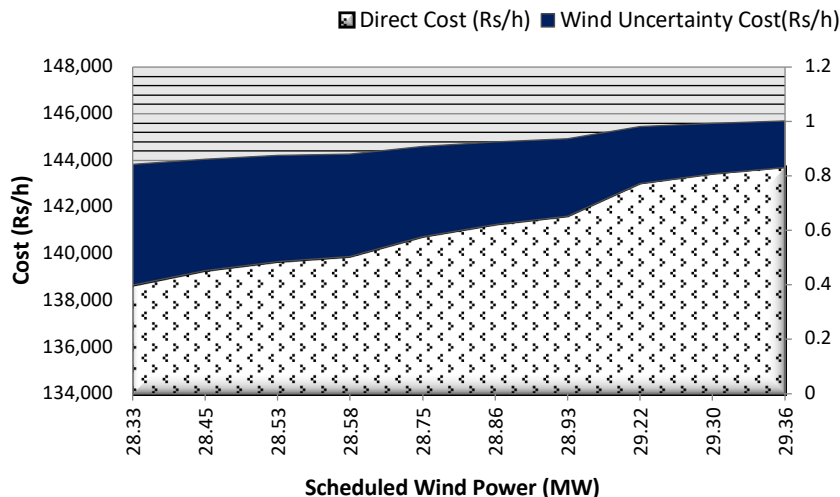


Fig. 4 Variation of wind power costs (Rs/h) with wind scheduled power (MW)

**Table 7**

Solution of power scheduling problem with three thermal generators and two wind generators using ACSM

Output Variables	200 MW	225 MW	250 MW	275 MW	300 MW
$P_{T1}$ (MW)	48.15	56.88	65.10	73.66	82.46
$P_{T2}$ (MW)	47.80	56.51	64.72	73.27	82.22
$P_{T3}$ (MW)	48.12	56.85	65.07	73.63	82.88
$P_{w1}$ (MW)	28.53	28.32	28.74	28.85	28.45
$P_{w2}$ (MW)	29.21	28.92	29.29	29.35	28.57
BCS fuel cost - Gt1 (Rs/h)	496.37	571.85	643.19	717.80	794.78
BCS fuel cost - Gt2 (Rs/h)	619.05	678.42	734.88	794.26	857.03
BCS fuel cost - Gt3 (Rs/h)	548.67	614.50	677.31	743.59	816.20
BCS total fuel cost (Rs/h)	1,664.10	1,864.77	2,055.40	2,255.66	2,468.02
BCS $NO_x$ emission (kg/h) - Gt1	77.20	79.67	82.87	87.12	92.45
BCS $NO_x$ Emission (kg/h) - Gt2	5.86	4.86	4.83	5.72	7.67
BCS $NO_x$ emission (kg/h) - Gt3	45.89	48.14	51.12	55.12	60.45
BCS total $NO_x$ emission (kg/h)	128.95	132.68	138.83	147.97	160.58
BCS $SO_2$ emission (kg/h) - Gt1	297.78	343.06	385.85	430.60	476.77
BCS $SO_2$ emission (kg/h) - Gt2	371.43	407.05	440.93	476.55	514.22
BCS $SO_2$ emission (kg/h) - Gt3	329.20	368.70	406.39	446.15	489.72
BCS total $SO_2$ emission (kg/h)	998.42	1,118.81	1,233.17	1,353.31	1,480.71
Direct cost $P_{w1}$ (Rs/h)	139,668.70	138,656.40	140,722.40	141,245.70	139,272.50
Direct cost $P_{w2}$ (Rs/h)	143,014.80	141,608.80	143,419.00	143,706.10	139,877.90
Total direct Cost (Rs/h)	282,683.50	280,265.20	284,141.40	284,951.80	279,150.40
Wind uncertainty cost $P_{w1}$ (Rs/h)	4,537.79	5,177.48	3,871.99	3,541.31	4,788.18
Wind uncertainty cost $P_{w2}$ (Rs/h)	2,423.42	3,311.86	2,168.06	1,986.61	4,405.62
Total uncertainty cost (Rs/h)	6,961.21	8,489.34	6,040.05	5,527.92	9,193.80
Total cost (Rs/h) - Gw1	144,206.50	143,833.90	144,594.40	144,787.01	144,060.78
Total cost (Rs/h) - Gw2	145,438.20	144,920.70	145,587.06	145,692.71	144,283.52
Total wind generation cost (Rs/h)	289,644.71	288,754.60	290,181.46	290,479.72	288,344.30
Transmission losses (MW)	1.75	2.30	2.91	3.64	4.47
Simulation time (sec)	0.72	0.72	0.73	0.73	0.73

**Table 8**

Solution of power scheduling problem with three thermal generators, one solar unit and one wind generator using ACSM

Output variables	200 MW	225 MW	250 MW	275 MW	300 MW
$P_{T1}$ (MW)	48.17	57.51	65.07	73.37	81.90
$P_{T2}$ (MW)	47.96	56.10	64.70	73.94	82.48
$P_{T3}$ (MW)	48.54	55.93	65.04	73.33	81.85
$P_s$ (MW)	29.75	29.38	29.40	29.45	29.51
$P_w$ (MW)	27.44	28.11	28.85	28.59	28.71
BCS fuel cost - Gt1 (Rs/h)	496.55	577.34	642.97	715.30	789.89
BCS fuel cost - Gt2 (Rs/h)	620.17	675.62	734.70	798.92	858.82
BCS fuel cost - Gt3 (Rs/h)	551.80	607.47	677.11	741.21	808.06
BCS total fuel cost (Rs/h)	1,668.53	1,860.44	2,054.79	2,255.44	2,456.79
BCS $NO_x$ emission (kg/h) - Gt1	77.20	79.88	82.86	86.96	92.08
BCS $NO_x$ emission (kg/h) - Gt2	5.83	4.89	4.83	5.83	7.74
BCS $NO_x$ emission (kg/h) - Gt3	45.97	47.86	51.11	54.96	59.80
BCS total $NO_x$ emission (kg/h)	129.01	132.64	138.81	147.76	159.64
BCS $SO_2$ emission (kg/h) - Gt1	297.89	346.35	385.71	429.10	473.83
BCS $SO_2$ emission (kg/h) - Gt2	372.10	405.37	440.82	479.35	515.29
BCS $SO_2$ emission(kg/h)- Gt3	331.08	364.48	406.27	444.73	484.84
BCS total $SO_2$ emission (kg/h)	1,001.08	1,116.21	1,232.81	1,353.18	1,473.97
Direct cost of $P_s$ (Rs/h)	148,755.25	146,935.95	147,030.00	147,287.60	147,579.60
Solar uncertainty cost $P_s$ (Rs/h)	-2,280.24	-460.94	-555.01	-812.59	-1,104.59
Total solar generation cost (Rs/h)	146,475.00	146,475.00	146,474.99	146,475.00	146,475.00
Direct cost of $P_w$ (Rs/h)	134,354.60	137,618.20	141,236.00	139,950.90	140,576.30
Wind uncertainty cost of $P_w$ (Rs/h)	7,895.74	5,833.52	3,547.43	4,359.47	3,964.32
Total wind generation cost (Rs/h)	142,250.40	143,451.70	144,783.50	144,310.40	144,540.60
Total direct cost (Rs/h)	283,109.85	284,554.15	288,266.00	287,238.50	288,155.88
Total uncertainty cost (Rs/h)	5,615.49	5,372.58	2,992.42	3,546.87	2,859.73
Total solar & wind gen. cost (Rs/h)	288,725.40	289,926.70	291,258.49	290,785.40	291,015.60
Transmission losses (MW)	1.74	2.28	2.90	3.64	4.47
Simulation time (sec)	0.91	0.92	0.92	0.93	0.93

#### 5.4 Test System 4

In this system, solar-wind-thermal power scheduling is performed. This system consists of total five generators i.e. three thermal generators, one solar unit and one wind

farm. Specifications of all the generators, environmental conditions and power demands are same as taken in previous test systems. All the output variables of Table 8 are calculated in the similar manner and by using same equations as discussed earlier. Transmission losses are

calculated separately for thermal, wind and solar power systems by using Eq. (20) to Eq. (22) respectively. Total transmission losses are calculated from Eq. (23).

Table 8 depicts the results of this system. Uncertainty costs of both solar and wind systems are calculated separately and then added to get total uncertainty cost. Similarly, direct cost of the system is evaluated. The sum of total direct cost and uncertainty cost gives overall cost of renewable power. While doing scheduling of renewable power, care has been taken to have full advantage of these resources. That is by proper load sharing the fuel costs and emission pollutants can be reduced.

### 5.5 Test system 5

In this system, four thermal generators are considered initially. Then in each step, few of them are replaced by solar/wind or solar & wind generators. For each new set, the fuel costs & emissions are evaluated (without changing power demand, total number of generators and atmospheric conditions). The variation in fuel costs and emissions with the reduction in the number of thermal generators is obtained. For this, the following four cases are observed:

- Case I. All four thermal generators are used
- Case II. One thermal generator is replaced by one solar unit
- Case III. One thermal generator is replaced by one wind farm
- Case IV. Two thermal generators are replaced by one solar unit and one wind farm.

All the required data and conditions used for this system are same as used in previous test systems. In the first case, all four thermal generators of Table 1 are used. In second and third cases last thermal generator of the Table 1 is replaced by solar unit/wind farm, one by one. In fourth case, the bottom two generators of Table 1 are replaced by one solar unit and one wind farm. Fuel costs and emissions are found out for all four cases and all the observations are put down in Table 9. Power demand is considered as 400 MW.

Fig. 5 as well as the results that came from the first case to the last shows a decline in the values of fuel costs and  $SO_2$  emissions. As the power available for the wind system (30 MW) is slightly more than the power of solar system (29.295 MW), so powers are scheduled to

individual systems accordingly. Due to this, a very small difference in fuel costs is appearing in case II and case III. In case IV, solar and wind systems has shared 59.20593 MW power load by replacing two thermal generators. So, the difference between fuel cost and  $SO_2$  emissions is more as compared to the previous cases.

Therefore it is proved that the values of fuel cost (4067.98 Rs/h) and  $SO_2$  emission (2,441.05 kg/h) reduced to 3,232.94 Rs/h and 1,939.30 kg/h, respectively, when number of thermal generators reduced from four to two, in this test system.

## 6. Comparisons

In this paper, values of direct cost coefficients of wind are taken lesser than the direct cost coefficients of solar system. After comparing the results of test systems 2, 3, and 4, it seems that for almost similar power scheduling, wind generation is better in terms of overall cost. But few technical problems tend to limit its attractiveness. For instance, it is an intermittent source of energy which generates variable powers. Therefore, it must be used along with other appropriate power generation system. Also, coefficients of solar, wind uncertainty costs and direct costs can vary from state to state in the same country, so their tariffs will also vary.

In test system 5, it has been proved that fuel costs and emissions depend upon the number of thermal generators. For the same demand and total number of generators, if number of thermal generators are reduced, the fuel costs and  $SO_2$  emissions drastically fall in their respective values. Even now renewable power has been put in a very small quantity as compared to the thermal power, yet its effect is prominent, as described in this paper. Therefore, RER needs to be utilized in more quantity and more wisely. This will reduce the use of fossil fuels in power generation system gradually.

RER are the lowest cost source of power generation in most parts of the world. Average electricity cost of solar generation has fallen into fossil fuel cost range globally from 2014 onwards. In many states of India, costs of solar/wind systems are lesser than thermal power systems too. Solar project like Rewa (750 MW, Madhya Pradesh, India) and wind project like Muppandal (1500 MW, Tamil Nadu, India) are being encouraged due to low solar/ wind power costs in India.

**Table 9**  
Solution of composite system using ACSM

Output variables	Case I	Case II	Case III	Case IV
$P_{T1}$ (MW)	102.06	137.19	136.58	178.92
$P_{T2}$ (MW)	101.85	137.70	137.48	178.78
$P_{T3}$ (MW)	101.67	136.60	137.43	–
$P_{T4}$ (MW)	102.23	–	–	–
$P_s$ (MW)	–	29.16	–	29.25
$P_w$ (MW)	–	–	29.47	29.94
Total fuel cost (Rs/h)	4,067.98	3,798.65	3,798.51	3,232.93
Total $NO_x$ emission (kg/h)	633.31	302.89	302.91	309.87
Total $SO_2$ emission (kg/h)	2,441.05	2,278.92	2,278.84	1,939.30

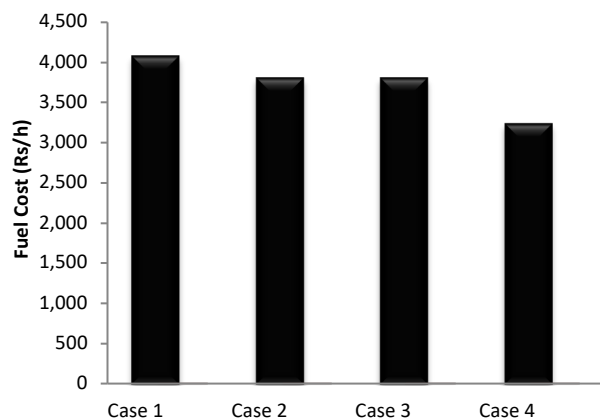


Fig. 5 Variation of fuel costs with each case for test system 5

## 7. Conclusion

In this paper, a multi-objective solar-wind-thermal power scheduling problem was designed, which simultaneously satisfies economic (fuel cost and operating costs of RER system) and emission ( $NO_x$  &  $SO_2$ ) constraints. The problem was optimized by using ACSM and the results are collated with SM.

The wind data was discerned with Weibull Distribution Density Function. The solar data of New Delhi (India) was considered for the framed scheduling problem. The available power of RER system depends upon topography and meteorology of the considered place, which is evaluated as 29.295 MW (for solar system) and 30 MW (for wind system), for the scrutinized conditions. On the basis of the value of available power, a remarkable decline is observed in the value of fuel cost. It was found 2117.36 Rs/h (for purely thermal system), 1656.71 Rs/h (for solar-thermal system), 1664.10 Rs/h (for wind-thermal system) and 1668.53 Rs/h (for solar-wind-thermal system), for 200 MW power demand. Similar turn down is noted in the values of emissions ( $NO_x$  &  $SO_2$ ). To reduce the intermittency of RER based power system, the adequate permutations of generating units (RER and thermal system) are required. The solution of the suggested model demonstrates that the undetermined behavior of RER based power systems is lessened for the integrated systems.

The outcomes of the presented problem intelligibly represent the primacy of ACSM over SM. The values of fuel cost, emissions ( $NO_x$  &  $SO_2$ ), transmission losses and simulation time are observed as 2319.35 Rs/h, 151.31kg/h & 1391.52 kg/h, 3.55 kg/h and 0.51sec, respectively, when the problem is examined by using ACSM (for 225 MW power demand). When the same problem is inspected with SM the values of these variables are obtained as 2,321.67 Rs/h, 151.47 kg/h, 1,392.91kg/h, 3.56 MW and 0.60 sec. The better out-turns have proved that the ACSM is a powerful tool for solving constrained optimization problems. For decision making, fuzzy cardinal priority ranking of non-dominating solutions was used. Its amalgamation with ACSM provides fine precision and solidity to the system to yield high computational efficiencies.

## Acknowledgment

I.K. Gujral Punjab Technical University, Kapurthala 144603, Punjab, India is gratefully acknowledged for the expertise and throughout assistance in all aspects of this research.

## References

- Brar, Y.S., Dhillon, J.S., & Kothari, D.P. (2005). Fuzzy satisfying multi-objective generation scheduling based on simplex weightage pattern search. *International Journal of Electrical Power & Energy Systems*, 27(7), 518-527; <https://doi.org/10.1016/j.ijepes.2005.06.002>
- Correa-Julian, C., Droguett, E.L., & Cardemil, J.M. (2020). Operation scheduling in a solar thermal system: A reinforcement learning - based framework. *Applied Energy*, 268, 11943; <https://doi.org/10.1016/j.apenergy.2020.114943>
- Damodaran, S.K., & Kumar, T.K.S. (2018). Hydro-thermal-wind generation scheduling considering economic and environmental factors using heuristic algorithms. *Energies*, 11(2), 353; <https://doi.org/10.3390/en11020353>
- Deb, K. (2005). *Optimization for Engineering Design: Algorithms and Examples*, 2nd ed. PHI, New Delhi, India; ISBN-978-81-203-4678-9.
- Dhillon, J.S., Parti, S.C., & Kothari, D.P. (2002). Fuzzy decision making in stochastic multi-objective short term hydrothermal scheduling. *IEEE Proceedings - Generation, Transmission and Distribution*, 149(2), 191-200; <http://dx.doi.org/10.1049/ip-gtd:20020176>
- Dubey, H.M., Pandit, M., & Panigrahi, B.K. (2015a). Hybrid flower pollination algorithm with time-varying fuzzy selection mechanism for wind integrated multi-objective dynamic economic dispatch. *Renewable Energy*, 83, 188-202; <https://doi.org/10.1016/j.renene.2015.04.034>
- Dubey, H.M., Pandit, M., & Panigrahi, B.K. (2015b). A biologically inspired modified flower pollination algorithm for solving economic dispatch problems in modern power systems. *Cognitive Computation*, 7, 594-608; <https://doi.org/10.1007/s12559-015-9324-1>
- Gangwar, A.K., & Chishti, F. (2014). Hybrid simplex method for economic load dispatch. *Advanced Research in Electrical and Electronic Engineering*, 1(3), 51-57.
- He, Z., Zhou, J., Sun, N., Jia, B., & Qin, H. (2019). Integrated scheduling of hydro, thermal and wind power with spinning reserve. *Energy Procedia*, 158, 6302-6308; <https://doi.org/10.1016/j.egypro.2019.01.409>
- Hetzer, J., Yu, D.C., & Bhattarai, K. (2008). An economic dispatch model incorporating wind power. *IEEE Transactions on Energy Conversion*, 23(2), 603-611; <https://doi.org/10.1109/TEC.2007.914171>
- Kayalvizhi, S., & Kumar, D.M.V. (2018). Stochastic optimal power flow in presence of wind generations using harmony search algorithm, *Proceedings of the 20th National Power Systems Conference, Dec. 14-16.NIT Tiruchirappalli, India*; <http://doi.org/10.1109/NPSC.2018.8771822>
- Kothari, D.P., & Dhillon, J.S. (2011). *Power System Optimization. 2nd ed.* PHI, New Delhi, India.
- Li, F., & Kuri, B. (2005). Generation scheduling in a system with wind power. 2005 IEEE/PES Transmission and Distribution Conference & Exhibition: Asia and Pacific, August 18, 2005, Dalian China, 1-6; <http://doi.org/10.1109/TDC.2005.1547157>
- Mayo, W.E. (1995). *Programming with Fortran 77*. McGraw-Hill.
- Mohamed, M., Youssef, A., Ebeed, M., & Kamel, S. (2019). Hybrid optimization technique for short term wind-solar-hydrothermal generation scheduling. *IEEE Conference on Power Electronics and Renewable Energy (CPERE)*, Aswan

- City, Egypt, pp. 212-216; <https://doi.org/10.1109/CPERE45374.2019.8980237>
- Mondal, S., Bhattacharya, A., & Halder, S. (2012). Solution of cost constrained emission dispatch problems considering wind power generation using gravitational search algorithm. *IEEE-International Conference on Advances in Engineering, Science and Management (ICAESM-2012)*, Nagapattinam, Tamil Nadu, India, 169-174.
- Mondal, S., Bhattacharya, A., & Dey, S.H.N. (2013). Multi-objective economic emission load dispatch solution using gravitational search algorithm and considering wind power penetration. *International Journal of Electrical Power and Energy Systems*, 44(1), 282-292; <https://doi.org/10.1016/j.ijepes.2012.06.049>
- Nguyen, T.T., Pham, L.H., Mohammadi, F., & Kien, L.C. (2020). Optimal scheduling of large scale wind-hydro-thermal systems with fixed-head short-term model. *Applied Sciences*, 10(8), 2964; <https://doi.org/10.3390/app10082964>
- Panda, A., & Tripathy, M. (2016). Solution of wind integrated thermal generation system for environmental optimal power flow using hybrid algorithm, *Journal of Electrical Systems and Information Technology*, 3(2), 151-160; <https://doi.org/10.1016/j.jesit.2016.01.004>
- Reddy, S.S. (2017a). Optimal scheduling of wind-thermal power system using clustered adaptive teaching learning based optimization. *Electrical Engineering*, 99, 535-550; <https://doi.org/10.1007/s00202-016-0382-5>
- Reddy, S.S. (2017b). Optimization of renewable energy resources in hybrid energy systems. *Journal of Green Engineering*, 7(1&2), 43-60; <https://doi.org/10.13052/jge1904-4720.7123>
- Reddy, S.S., Abhyankar, A.R., Bijwe, P.R. (2011). Multi-objective day ahead real power market clearing with voltage dependent load models. *International Journal of Emerging Electric Power Systems*, 12(4); <https://doi.org/10.2202/1553-779X.2727>
- Reddy, S.S., Abhyankar, A.R., & Bijwe, P.R. (2015). Co-optimization of energy and demand-side reserves in day-ahead electricity markets. *International Journal of Emerging Electric Power Systems*, 16(2), 195-206; <https://doi.org/10.1515/ijepes-2014-0020>
- Reddy, S.S., Park, J.Y., & Jung, C.M. (2016). Optimal operation of microgrid using hybrid differential evolution and harmony search algorithm. *Frontiers in Energy*, 10(3), 355-362; <https://doi.org/10.1007/s11708-016-0414-x>
- Saxena, N., & Ganguli, S. (2015). Solar and wind power estimation and economic load dispatch using firefly algorithm. *Procedia Computer Science*, 70, 688-700; <https://doi.org/10.1016/j.procs.2015.10.106>
- Singal, R.K. (2009). *Non-Conventional Energy Resources*, 2<sup>nd</sup> ed., S.K. Kataria & Sons, New Delhi India. ISBN-8188458821
- Sinha, N., Chakrabarti, R., & Chattopadhyay, P.K. (2003). Evolutionary programming techniques for economic load dispatch. *IEEE Transactions on Evolutionary Computation*, 7(1), 83-93; <http://doi.org/10.1109/TEVC.2002.806788>
- Takahama, T., & Sakai, S. (2005). Constrained optimization by applying the /spl alpha/ constrained method to the nonlinear simplex method with mutations. *IEEE Transactions on Evolutionary Computation*, 9(5), 437-450; <http://doi.org/10.1109/TEVC.2005.850256>
- Tan, S., Wang, X., & Jiang, C. (2019). Optimal scheduling of hydro-PV-Wind hybrid system considering CHP and BESS coordination. *Applied Sciences*, 9(5) 892; <https://doi.org/10.3390/app9050892>
- Tyagi, N., Dubey, H.M., & Pandit, M. (2016). Economic load dispatch of wind-solar-thermal system using backtracking search algorithm. *International Journal of Engineering, Science and Technology*, 8(4), 16-27; <http://dx.doi.org/10.4314/ijest.v8i4.3>
- Vaderobli, A., Parikh, D., & Diwerkar, U. (2020). Optimization under uncertainty to reduce the cost of energy for parabolic trough solar power plants for different weather conditions. *Energies*, 13(12), 3131; <https://doi.org/10.3390/en13123131>
- Wood, A.J., & Wollenberg, B.F. (2006). *Power Generation, Operation, and Control*, 2<sup>nd</sup> ed., Wiley, India. ISBN 978-81-265-0838-9



©2021. This article is an open access article distributed under the terms and conditions of the Creative Commons Attribution-ShareAlike 4.0 (CC BY-SA) International License (<http://creativecommons.org/licenses/by-sa/4.0/>)